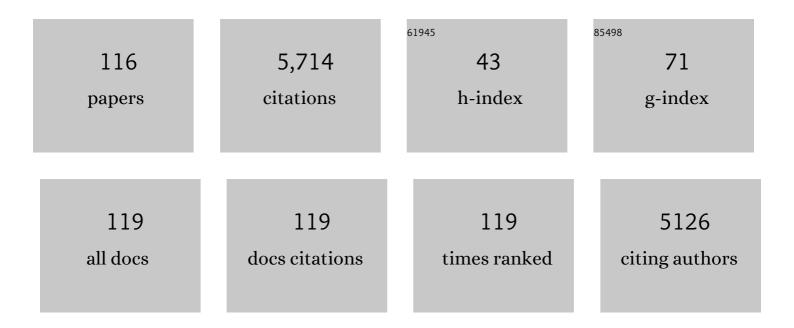
Christine V Putnis

List of Publications by Year in descending order

Source: https://exaly.com/author-pdf/6259207/publications.pdf Version: 2024-02-01



#	Article	IF	CITATIONS
1	<i>In situ</i> observations of the occlusion of a clay-sugar compound within calcite. Environmental Science: Nano, 2022, 9, 523-531.	2.2	6
2	Dynamic force spectroscopy for quantifying single-molecule organo–mineral interactions. CrystEngComm, 2021, 23, 11-23.	1.3	8
3	Nanoscale imaging of the simultaneous occlusion of nanoplastics and glyphosate within soil minerals. Environmental Science: Nano, 2021, 8, 2855-2865.	2.2	11
4	Face-Specific Occlusion of Lipid Vesicles within Calcium Oxalate Monohydrate. Crystal Growth and Design, 2021, 21, 2398-2404.	1.4	8
5	Facet-Specific Dissolution–Precipitation at Struvite–Water Interfaces. Crystal Growth and Design, 2021, 21, 4111-4120.	1.4	8
6	Relative rates of fluid advection, elemental diffusion and replacement govern reaction front patterns. Earth and Planetary Science Letters, 2021, 565, 116950.	1.8	7
7	Nanoparticles formed during mineral-fluid interactions. Chemical Geology, 2021, 586, 120614.	1.4	13
8	Molecular Understanding of Humic Acid-Limited Phosphate Precipitation and Transformation. Environmental Science & Technology, 2020, 54, 207-215.	4.6	46
9	Direct imaging of coupled dissolution-precipitation and growth processes on calcite exposed to chromium-rich fluids. Chemical Geology, 2020, 552, 119770.	1.4	15
10	Phosphorylated/Nonphosphorylated Motifs in Amelotin Turn Off/On the Acidic Amorphous Calcium Phosphate-to-Apatite Phase Transformation. Langmuir, 2020, 36, 2102-2109.	1.6	12
11	Dissolution and Precipitation Dynamics at Environmental Mineral Interfaces Imaged by In Situ Atomic Force Microscopy. Accounts of Chemical Research, 2020, 53, 1196-1205.	7.6	33
12	Editorial for Special Issue "Mineral Surface Reactions at the Nanoscale― Minerals (Basel,) Tj ETQq0 0 0 rgBT	/Overlock	19 Tf 50 302
13	Inhibition of Spiral Growth and Dissolution at the Brushite (010) Interface by Chondroitin 4-Sulfate. Journal of Physical Chemistry B, 2019, 123, 845-851.	1.2	7
14	Molecular-Scale Investigations Reveal Noncovalent Bonding Underlying the Adsorption of Environmental DNA on Mica. Environmental Science & Technology, 2019, 53, 11251-11259.	4.6	26
15	Direct Observations of the Occlusion of Soil Organic Matter within Calcite. Environmental Science & Technology, 2019, 53, 8097-8104.	4.6	35
16	Direct Observations of the Coupling between Quartz Dissolution and Mg-Silicate Formation. ACS Earth and Space Chemistry, 2019, 3, 617-625.	1.2	2
17	Underlying Role of Brushite in Pathological Mineralization of Hydroxyapatite. Journal of Physical Chemistry B, 2019, 123, 2874-2881.	1.2	23

¹⁸Humic Acids Limit the Precipitation of Cadmium and Arsenate at the Brushiteâ€"Fluid Interface.
Environmental Science & Environmental Science &

#	Article	IF	CITATIONS
19	Timescales of interface-coupled dissolution-precipitation reactions on carbonates. Geoscience Frontiers, 2019, 10, 17-27.	4.3	34
20	Baryte cohesive layers formed on a (010) gypsum surface by a pseudomorphic replacement. European Journal of Mineralogy, 2019, 31, 289-299.	0.4	5
21	Mineral reactivity: from biomineralization and Earth's climate evolution, to CO2 capture and monument conservation. European Journal of Mineralogy, 2019, 31, 205-207.	0.4	Ο
22	Direct Observation of Simultaneous Immobilization of Cadmium and Arsenate at the Brushite–Fluid Interface. Environmental Science & Technology, 2018, 52, 3493-3502.	4.6	21
23	Peridotite weathering is the missing ingredient of Earth's continental crust composition. Nature Communications, 2018, 9, 634.	5.8	36
24	Mechanisms of Modulation of Calcium Phosphate Pathological Mineralization by Mobile and Immobile Small-Molecule Inhibitors. Journal of Physical Chemistry B, 2018, 122, 1580-1587.	1.2	20
25	Atomic force microscopy imaging of classical and nonclassical surface growth dynamics of calcium orthophosphates. CrystEngComm, 2018, 20, 2886-2896.	1.3	10
26	Sequestration of Antimony on Calcite Observed by Time-Resolved Nanoscale Imaging. Environmental Science & Technology, 2018, 52, 107-113.	4.6	23
27	Metal Sequestration through Coupled Dissolution–Precipitation at the Brucite–Water Interface. Minerals (Basel, Switzerland), 2018, 8, 346.	0.8	21
28	Interfacial Precipitation of Phosphate on Hematite and Goethite. Minerals (Basel, Switzerland), 2018, 8, 207.	0.8	25
29	Dynamics and Molecular Mechanism of Phosphate Binding to a Biomimetic Hexapeptide. Environmental Science & Technology, 2018, 52, 10472-10479.	4.6	9
30	The replacement of a carbonate rock by fluorite: Kinetics and microstructure. American Mineralogist, 2017, 102, 126-134.	0.9	25
31	Siderite dissolution coupled to iron oxyhydroxide precipitation in the presence of arsenic revealed by nanoscale imaging. Chemical Geology, 2017, 449, 123-134.	1.4	27
32	Mineral Surface Rearrangement at High Temperatures: Implications for Extraterrestrial Mineral Grain Reactivity. ACS Earth and Space Chemistry, 2017, 1, 113-121.	1.2	7
33	Halide-Dependent Dissolution of Dicalcium Phosphate Dihydrate and Its Modulation by an Organic Ligand. Crystal Growth and Design, 2017, 17, 3868-3876.	1.4	2
34	Energetic Basis for Inhibition of Calcium Phosphate Biomineralization by Osteopontin. Journal of Physical Chemistry B, 2017, 121, 5968-5976.	1.2	11
35	In Situ Atomic Force Microscopy Imaging of Octacalcium Phosphate Crystallization and Its Modulation by Amelogenin's C-Terminus. Crystal Growth and Design, 2017, 17, 2194-2202.	1.4	14
36	Imaging Organophosphate and Pyrophosphate Sequestration on Brucite by in Situ Atomic Force Microscopy. Environmental Science & Technology, 2017, 51, 328-336.	4.6	21

#	Article	IF	CITATIONS
37	Effect of ferrous iron on the nucleation and growth of CaCO ₃ in slightly basic aqueous solutions. CrystEngComm, 2017, 19, 447-460.	1.3	19

Hydration Effects on the Stability of Calcium Carbonate Pre-Nucleation Species. Minerals (Basel,) Tj ETQq0 0 0 rgBT $_{0.8}^{-10}$ Verlock 10 Tf 50 7

39	Influence of pH and citrate on the formation of oxalate layers on calcite revealed by in situ nanoscale imaging. CrystEngComm, 2017, 19, 3420-3429.	1.3	14
40	Direct Observation of Spiral Growth, Particle Attachment, and Morphology Evolution of Hydroxyapatite. Crystal Growth and Design, 2016, 16, 4509-4518.	1.4	43
41	A potentiometric study of the performance of a commercial copolymer in the precipitation of scale forming minerals. CrystEngComm, 2016, 18, 5744-5753.	1.3	7
42	Exploring the effect of poly(acrylic acid) on pre- and post-nucleation BaSO ₄ species: new insights into the mechanisms of crystallization control by polyelectrolytes. CrystEngComm, 2016, 18, 2830-2842.	1.3	24
43	Porosity generated during the fluid-mediated replacement of calcite by fluorite. CrystEngComm, 2016, 18, 6867-6874.	1.3	14
44	In Situ Nanoscale Imaging of Struvite Formation during the Dissolution of Natural Brucite: Implications for Phosphorus Recovery from Wastewaters. Environmental Science & Technology, 2016, 50, 13032-13041.	4.6	65
45	Hydration effects on gypsum dissolution revealed by in situ nanoscale atomic force microscopy observations. Geochimica Et Cosmochimica Acta, 2016, 179, 110-122.	1.6	23
46	The pseudomorphic replacement of marble by apatite: The role of fluid composition. Chemical Geology, 2016, 425, 1-11.	1.4	27
47	Control of silicate weathering by interface-coupled dissolution-precipitation processes at the mineral-solution interface. Geology, 2016, 44, 567-570.	2.0	68
48	Visualizing Organophosphate Precipitation at the Calcite–Water Interface by in Situ Atomic-Force Microscopy. Environmental Science & Technology, 2016, 50, 259-268.	4.6	15
49	Direct Nanoscale Imaging Reveals the Growth of Calcite Crystals via Amorphous Nanoparticles. Crystal Growth and Design, 2016, 16, 1850-1860.	1.4	89
50	Removal of Fe(II) from groundwater via aqueous portlandite carbonation and calcite-solution interactions. Chemical Engineering Journal, 2016, 283, 404-411.	6.6	17
51	Mechanistic Principles of Barite Formation: From Nanoparticles to Micron-Sized Crystals. Crystal Growth and Design, 2015, 15, 3724-3733.	1.4	43
52	Experimental study of the replacement of calcite by calcium sulphates. Geochimica Et Cosmochimica Acta, 2015, 156, 75-93.	1.6	30
53	In situ Imaging of Interfacial Precipitation of Phosphate on Goethite. Environmental Science & Technology, 2015, 49, 4184-4192.	4.6	56
54	Interactions of arsenic with calcite surfaces revealed by in situ nanoscale imaging. Geochimica Et Cosmochimica Acta, 2015, 159, 61-79.	1.6	60

#	Article	IF	CITATIONS
55	The influence of pH on barite nucleation and growth. Chemical Geology, 2015, 391, 7-18.	1.4	48
56	Direct nanoscale observations of the coupled dissolution of calcite and dolomite and the precipitation of gypsum. Beilstein Journal of Nanotechnology, 2014, 5, 1245-1253.	1.5	30
57	Coupled fluctuations in element release during dolomite dissolution. Mineralogical Magazine, 2014, 78, 1355-1362.	0.6	22
58	The effect of a copolymer inhibitor on baryte precipitation. Mineralogical Magazine, 2014, 78, 1423-1430.	0.6	9
59	Textural Evolution of Plagioclase Feldspar across a Shear Zone: Implications for Deformation Mechanism and Rock Strength. Journal of Petrology, 2014, 55, 1457-1477.	1.1	62
60	Coupled dissolution and precipitation at mineral–fluid interfaces. Chemical Geology, 2014, 383, 132-146.	1.4	290
61	Direct Observations of the Dissolution of Fluorite Surfaces with Different Orientations. Crystal Growth and Design, 2014, 14, 69-77.	1.4	14
62	Modelling the effects of salt solutions on the hydration of calcium ions. Physical Chemistry Chemical Physics, 2014, 16, 7772-7785.	1.3	54
63	The Mineral-Water Interface: Where Minerals React with the Environment. Elements, 2013, 9, 177-182.	0.5	116
64	Selenium incorporation into calcite and its effect on crystal growth: An atomic force microscopy study. Chemical Geology, 2013, 340, 151-161.	1.4	57
65	Influence of chemical and structural factors on the calcite–calcium oxalate transformation. CrystEngComm, 2013, 15, 9968.	1.3	22
66	Direct observations of the influence of solution composition on magnesite dissolution. Geochimica Et Cosmochimica Acta, 2013, 109, 113-126.	1.6	13
67	An atomic force microscopy study of the dissolution of calcite in the presence of phosphate ions. Geochimica Et Cosmochimica Acta, 2013, 117, 115-128.	1.6	42
68	Template-Assisted Crystallization of Sulfates onto Calcite: Implications for the Prevention of Salt Damage. Crystal Growth and Design, 2013, 13, 40-51.	1.4	16
69	Coupled Dissolution and Precipitation at the Cerussite-Phosphate Solution Interface: Implications for Immobilization of Lead in Soils. Environmental Science & Technology, 2013, 47, 13502-13510.	4.6	29
70	Dissolution and Carbonation of Portlandite [Ca(OH) ₂] Single Crystals. Environmental Science & Technology, 2013, 47, 11342-11349.	4.6	105
71	Sequestration of Selenium on Calcite Surfaces Revealed by Nanoscale Imaging. Environmental Science & Technology, 2013, 47, 13469-13476.	4.6	28
72	Mechanism of leached layer formation during chemical weathering of silicate minerals. Geology, 2012, 40, 947-950.	2.0	127

#	Article	IF	CITATIONS
73	Direct Nanoscale Observations of CO ₂ Sequestration during Brucite [Mg(OH) ₂] Dissolution. Environmental Science & Technology, 2012, 46, 5253-5260.	4.6	97
74	Kinetics of Calcium Phosphate Nucleation and Growth on Calcite: Implications for Predicting the Fate of Dissolved Phosphate Species in Alkaline Soils. Environmental Science & Technology, 2012, 46, 834-842.	4.6	92
75	In situ nanoscale observations of the dissolution of dolomite cleavage surfaces. Geochimica Et Cosmochimica Acta, 2012, 80, 1-13.	1.6	53
76	Posner's cluster revisited: direct imaging of nucleation and growth of nanoscale calcium phosphate clusters at the calcite-water interface. CrystEngComm, 2012, 14, 6252.	1.3	71
77	Direct observations of mineral fluid reactions using atomic force microscopy: the specific example of calcite. Mineralogical Magazine, 2012, 76, 227-253.	0.6	109
78	Direct observations of the modification of calcite growth morphology by Li+ through selectively stabilizing an energetically unfavourable face. CrystEngComm, 2011, 13, 3962.	1.3	20
79	Mineral replacement reactions in solid solution-aqueous solution systems: Volume changes, reactions paths and end-points using the example of model salt systems. Numerische Mathematik, 2011, 311, 211-236.	0.7	72
80	Ion-specific effects on the kinetics of mineral dissolution. Chemical Geology, 2011, 281, 364-371.	1.4	64
81	Effect of pH on calcite growth at constant ratio and supersaturation. Geochimica Et Cosmochimica Acta, 2011, 75, 284-296.	1.6	84
82	Specific effects of background electrolytes on the kinetics of step propagation during calcite growth. Geochimica Et Cosmochimica Acta, 2011, 75, 3803-3814.	1.6	57
83	Crystal growth of apatite by replacement of an aragonite precursor. Journal of Crystal Growth, 2010, 312, 2431-2440.	0.7	47
84	AFM study of the epitaxial growth of brushite (CaHPO4{middle dot}2H2O) on gypsum cleavage surfaces. American Mineralogist, 2010, 95, 1747-1757.	0.9	19
85	Crystal Growth and Dissolution of Calcite in the Presence of Fluoride Ions: An Atomic Force Microscopy Study. Crystal Growth and Design, 2010, 10, 60-69.	1.4	30
86	Interactions between Organophosphonate-Bearing Solutions and (101ì4) Calcite Surfaces: An Atomic Force Microscopy and First-Principles Molecular Dynamics Study. Crystal Growth and Design, 2010, 10, 3022-3035.	1.4	25
87	The experimental replacement of ilmenite by rutile in HCl solutions. Mineralogical Magazine, 2010, 74, 633-644.	0.6	53
88	The role of background electrolytes on the kinetics and mechanism of calcite dissolution. Geochimica Et Cosmochimica Acta, 2010, 74, 1256-1267.	1.6	128
89	The mechanism of cation and oxygen isotope exchange in alkali feldspars under hydrothermal conditions. Contributions To Mineralogy and Petrology, 2009, 157, 65-76.	1.2	86
90	Reaction induced fracturing during replacement processes. Contributions To Mineralogy and Petrology, 2009, 157, 127-133.	1.2	163

#	Article	IF	CITATIONS
91	The Control of Solution Composition on Ligand-Promoted Dissolution: DTPAâ^'Barite Interactions. Crystal Growth and Design, 2009, 9, 5266-5272.	1.4	14
92	An atomic force microscopy study of calcite dissolution in saline solutions: The role of magnesium ions. Geochimica Et Cosmochimica Acta, 2009, 73, 3201-3217.	1.6	99
93	An Atomic Force Microscopy Study of the Growth of a Calcite Surface as a Function of Calcium/Total Carbonate Concentration Ratio in Solution at Constant Supersaturation. Crystal Growth and Design, 2009, 9, 4344-4350.	1.4	52
94	Zircon coronas around Fe–Ti oxides: a physical reference frame for metamorphic and metasomatic reactions. Contributions To Mineralogy and Petrology, 2008, 156, 517-527.	1.2	48
95	Interaction between Epsomite Crystals and Organic Additives. Crystal Growth and Design, 2008, 8, 2665-2673.	1.4	23
96	Pseudomorphic replacement of single calcium carbonate crystals by polycrystalline apatite. Mineralogical Magazine, 2008, 72, 77-80.	0.6	42
97	The mechanism and kinetics of DTPA-promoted dissolution of barite. Applied Geochemistry, 2008, 23, 2778-2788.	1.4	60
98	An Atomic Force Microscopy study of the growth of calcite in the presence of sodium sulfate. Chemical Geology, 2008, 253, 243-251.	1.4	56
99	The effect of fluid composition on the mechanism of the aragonite to calcite transition. Mineralogical Magazine, 2008, 72, 111-114.	0.6	26
100	Macro- to nanoscale study of the effect of aqueous sulphate on calcite growth. Mineralogical Magazine, 2008, 72, 141-144.	0.6	2
101	The effect of cation:anion ratio in solution on the mechanism of barite growth at constant supersaturation: Role of the desolvation process on the growth kinetics. Geochimica Et Cosmochimica Acta, 2007, 71, 5168-5179.	1.6	105
102	An experimental study of the replacement of leucite by analcime. American Mineralogist, 2007, 92, 19-26.	0.9	104
103	The mechanism of reequilibration of solids in the presence of a fluid phase. Journal of Solid State Chemistry, 2007, 180, 1783-1786.	1.4	328
104	Hematite in porous red-clouded feldspars: Evidence of large-scale crustal fluid–rock interaction. Lithos, 2007, 95, 10-18.	0.6	114
105	In situ AFM study of the dissolution and recrystallization behaviour of polished and stressed calcite surfaces. Geochimica Et Cosmochimica Acta, 2006, 70, 1728-1738.	1.6	44
106	Interactions between mineral surfaces and dissolved species: From monovalent ions to complex organic molecules. Numerische Mathematik, 2005, 305, 791-825.	0.7	27
107	Direct observation of heavy metal-mineral association from the Clark Fork River Superfund Complex: Implications for metal transport and bioavailability. Geochimica Et Cosmochimica Acta, 2005, 69, 1651-1663.	1.6	169
108	Direct observations of pseudomorphism: compositional and textural evolution at a fluid-solid interface. American Mineralogist, 2005, 90, 1909-1912.	0.9	183

#	Article	IF	CITATIONS
109	Environmentally important, poorly crystalline Fe/Mn hydrous oxides: Ferrihydrite and a possibly new vernadite-like mineral from the Clark Fork River Superfund Complex. American Mineralogist, 2005, 90, 718-724.	0.9	101
110	An atomic force microscopy and molecular simulations study of the inhibition of barite growth by phosphonates. Surface Science, 2004, 553, 61-74.	0.8	48
111	A mechanism of mineral replacement: isotope tracing in the model system KCl-KBr-H2O. Geochimica Et Cosmochimica Acta, 2004, 68, 2839-2848.	1.6	99
112	The dissolution rates of natural glasses as a function of their composition at pH 4 and 10.6, and temperatures from 25 to 74°C. Geochimica Et Cosmochimica Acta, 2004, 68, 4843-4858.	1.6	321
113	Base-metals and organic content in stream sediments in the vicinity of a landfill. Applied Geochemistry, 2004, 19, 137-151.	1.4	20
114	The mechanism of fluid infiltration in peridotites at Almklovdalen, western Norway. Geofluids, 2002, 2, 203-215.	0.3	33
115	lon partitioning and element mobilization during mineral replacement reactions in natural and experimental systems. , 0, , 189-226.		2
116	Crystallization via Nonclassical Pathways: Nanoscale Imaging of Mineral Surfaces. ACS Symposium Series, 0, , 1-35.	0.5	3